Journal of the Nigerian Association of Mathematical Physics
Volume **19 (November, 2011), pp 369 – 386**

A theoretical parametric study of Water Flooding

Peter Ohirhian

Dept. of Petroleum Engineering, University of Benin,
Benin City, Edo State, Nigeria.

Abstract

A multidimensional mathematical model derived by combining equation of continuity and Darcy's law and solved using the strongly implicit procedure (SIP) has been used to study the effects of permeability distribution, shape of the relative permeability and capillary pressure curves, ratio of water to oil viscosity, and amount of connate water on the shape of the water saturation profiles, the time of water breakthrough and the cumulative oil recovery from a water flood project.

The effects of the various parameters on the oil recovery efficiency (the fraction of the initial oil in place that can be economically recovered) have been studied with respect to linear flow as well as for a five-spot pattern. The computer model described in this paper is capable of handling both patterns by mere alteration of the injection data.

The study shows that the parameters considered have much influence on the efficiency of oil recovery from a porous material.

1.0 Introduction

Since the accidental discovery of water flooding in the Pitthole City area, Western Pennsylvania [1], as a means of increasing the oil recovery, there have been numerous studies on how to maximize the amount of oil production from a given water flood project. These studies can be broadly classified as experimental, analytical, statistical or numerical.

Most experimental studies could not simulate the water saturation gradient behind the flood front. The more successful ones that overcame this problem were limited to homogenous systems. The investigators using the analytical tools derived mathematical equations that simulated the multiphase flow encountered in oil reservoirs. However, to solve the resulting equations, these investigators assumed common, regular geometric patterns. Most of these analytic techniques are even limited to homogenous reservoirs. More recently, statistical methods have been used to relate the oil recovery efficiency to such reservoir parameters as porosity, permeability, thickness, connate water saturation and oil viscosity. These correlations have been made by studying the reservoir at a specific geographical location. The probability that result obtained in this manner will apply well to reservoirs in other geographical locations is very small. The numerical techniques are the most versatile of the available methods. They are capable of relating oil recovery efficiency to all reservoir properties, water injection rates and injection well patterns.

In this study, the SIP technique developed by [4] for solving partial differential equations encountered in multidimensional heat conduction and introduced into the oil industry by [5] has been used to investigate the effects of permeability distribution, shape of the relative permeability and capillary pressure curves, the ratio of water-to-oil viscosity and the connate water saturation, on the shape of the water saturation profiles, the time of water breakthrough and the cumulative oil recovery from a water flood project. SIP is fast and insensitive to rounding errors in machine computations.. The ratio of water present in the slab plus water produced to the cumulative water injected (material balance check) was used as a criterion of accuracy of the five-spot pattern. For a water-to-oil viscosity, ratio of 1.5, material balance check on the porous slab used in this report varied between 1.006 and 0.9904 for a total injection of 0.16 pore volumes. The same slab was treated as a five-spot pattern in which water was injected at four corners and oil produced from the centre. Material balance figures were in the range on 1.0000 to 0.9994 for the same cumulative water injection of 0.16 pore volumes. By injecting water into al cells at one side of a five spot pattern and producing from all cells at the opposite side, the five spot pattern becomes a linear pattern. The accuracy of results from the computer model was further tested

with results from the linear model. The accuracy of a result from the linear case was determined by comparing the cumulative water injected into the system up to the time of breakthrough with that from Buckley-Leverett [2] model. There was a good agreement between both values.

Corresponding authors: Peter Ohirhian, E-mail: okuopet@gmail.com, Tel. +2348023394848

2.0 The Model

2.1 Equations of Two Phase Flow

The combination of Darcy's law and equation of continuity for simultaneous flow of water (denoted with subscript w) and oil (denoted by subscript o) yield the following equations[5]:

$$\nabla.\left\{\frac{[k]k_{rw}}{\mu_w}\rho_w\left(\nabla.P_w+\nabla.\ z\rho_w g\right)\right\}+\rho_w G_w=\phi\frac{\partial(S_w P_w)}{\partial t} \quad \text{..... ....} \quad (1a)$$

$$\nabla.\left\{\frac{[k]k_{ro}}{\mu_O}\rho_o\left(\nabla.P_O+\nabla.\ z\rho_O g\right)\right\}+\rho_O G_O=\phi\frac{\partial(S_O P_O)}{\partial t} \quad \text{..... ....} \quad (1\ b)$$

If we invoke an assumption of no phase transfer between all fluids present in the porous material[4], we have, for a two-dimensional system, the following equations:

$$\frac{\partial}{\partial x}\left\{\frac{[k]k_{rw}}{\mu_w B_w}\frac{\partial P_w}{\partial x}\right\}+\frac{\partial}{\partial y}\left\{\frac{[k]k_{rw}}{\mu_w B_w}\frac{\partial P_w}{\partial y}\right\}\pm Q_w=+\frac{\phi}{\beta_w}\frac{\partial S_w}{\partial P_c}\frac{\partial}{\partial t}(P_o-P_w) \quad \text{... (2 a)}$$

$$\frac{\partial}{\partial x}\left\{\frac{[k]k_{ro}}{\mu_o Bo}\frac{\partial Po}{\partial x}\right\}+\frac{\partial}{\partial y}\left\{\frac{[k]k_{ro}}{\mu_o B_o}\frac{\partial P_o}{\partial y}\right\}\pm Q_o=+\frac{\phi}{B_o}\frac{\partial Sw}{\partial P_c}\frac{\partial}{\partial t}(P_o-P_w) \quad (2\ b)$$

With initial conditions (I.Cs) as follows:

$P_w(x, y, 0) = CC_1$ atmosphères

$P_o(x, y, 0) = P_w(x, y, 0) + P(x, y, 0) = CC_1 atm + CC_2$ atm

Where Pw is the pressure in the water phase, Po, the pressure in the oil phase, Pc, the oil – water capillary pressure and CC_1 and CC_2 are specified constants. Where the initial value of water saturation is given, the corresponding Pc (x, y, 0) is computed by the computer program from the capillary pressure versus water saturation relation.

A closed boundary was imposed on all sides of slab. The resulting eight boundary conditions (B.Cs) can then be expressed as:

$$\left.\frac{\partial P_w}{\partial x}\right|_{i=1}=0 \quad (3a)$$

$$\left.\frac{\partial P_o}{\partial x}\right|_{i=1}=0 \quad (3b)$$

$$\left.\frac{\partial P_w}{\partial x}\right|_{i=I}=0 \quad (3c)$$

$$\left.\frac{\partial P_o}{\partial x}\right|_{i=I}=0 \quad (3d)$$

$$\left.\frac{\partial P_w}{\partial x}\right|_{j=1}=0 \quad (3e)$$

$$\left.\frac{\partial P_o}{\partial x}\right|_{j=1}=0 \quad (3f)$$

$$\left.\frac{\partial P_w}{\partial x}\right|_{j=J}=0 \quad (3g)$$

$$\left.\frac{\partial P_o}{\partial x}\right|_{j=J}=0 \quad (3h)$$

where I and J are the number of grid blocks in the x and y directions respectively.

2.2 Finite Difference approximation of Equations of Two Phase Flow

Difference operators were used to transform equations 2 a and 2 b to finite difference equations. The partial derivatives that occur in the left hand side of both equations was transformed to difference equations by the central difference operator defined by [3] as:

$$f' = \frac{f(x+h) - f(x-h)}{h}$$

The partial derivatives that occur in the right hand side of both equations was transformed to difference equations by the forward difference operator defined by [3] as:

$$f' = \frac{f(x+h) - f(x)}{h}$$

The finite difference of equation 2a is:

$$\left(\frac{Tw\,i-1/2,\,j}{\Delta x^2}\right) Pw\,i-1,\,j^{\,n+1} + \left(\frac{Twi,\,j-1/2}{\Delta y^2}\right) Pw\,i,\,ji-1^{\,n+1}$$

$$+ Pwi,\,j^{\,n+1} + \left[- \frac{Tw\,i-1/2,\,j}{\Delta x^2} - \frac{Twi,\,j-1/2}{\Delta y^2} - \frac{Tw\,i+1/2,\,j}{\Delta x^2} - \frac{Twi,\,j+1/2}{\Delta y^2} + \left(\frac{\Phi}{B_w}\,\frac{dS_w}{dP_c}\right)\frac{1}{\Delta t}\right]$$

$$+ \left(\frac{Tw\,i+1/2,\,j}{\Delta x^2}\right) Pw\,i+1,\,j^{\,n+1} + \left(\frac{Twi,\,j+1/2}{\Delta y^2}\right) Pwi,\,j^{\,n+1} - \left(\frac{\Phi}{B_w}\,\frac{dS_w}{dP_c}\right)\frac{1}{\Delta t}\,Po\,i,\;j^{\,n+1}$$

$$- \left(\frac{\Phi}{B_w}\,\frac{dS_w}{dP_c}\right)\frac{1}{\Delta t}\,Pw\,i,\;j^{\,n} + \left(\frac{\Phi}{B_w}\,\frac{dS_w}{dP_c}\right)\frac{1}{\Delta t}\,Po\,i,\;j^{\,n} + Qwi,\;j^{\,n+1} = 0 \quad \text{.....(2c)}$$

This equation can be written in compact form as:

$$BB_{wi,\,j}\,P_{wi,\,j-1}^{\,n+1} + DD_{wi,\,j}\,P_{wi-1,\,j}^{\,n+1} + EE_{wi,\,j}\,P_{wi,\,j}^{\,n+1}$$

$$+ FF_{wi,\,j}\,P_{wi+1,\,j}^{\,n+1} + HH_{wi,\,j}\;P_{wi,\,j+1}^{\,n+1k} - \left(\frac{\phi}{B_w}\frac{dS_w}{dP_c}\right)\frac{1}{\Delta t}\,P_{oi,\;j}^{\,n+1}$$

$$= 0 - \left(\frac{\phi}{B_w}\frac{dS_w}{dP_c}\right)\frac{1}{\Delta t}\,P_{wi\;,\,j}^{\,n} - \left(\frac{\phi}{B_w}\frac{dS_w}{dP_c}\right)\frac{1}{\Delta t}\,P_{oi\;,\,j}^{\,n} \quad \text{.....} \qquad (2d)$$

An equation similar 2d, can be written for the oil phase equation (2b).

The difference between the left and the right hand sides of equation 2d. for some assumed values of pressures that are not correct gives a finite residue, $R_w\,I\,,\,j$. Let us introduce an iteration counter, k. Also let us assume some values of pressure for the flow of water at the k^{th} iteration. If the assumed values of the pressure are not correct, there results a finite residue, $R_w\,I\,,\,j^{\,k}$. Then, equation 2d can be written as:

$$BB_{wi,j}P_{wi,j}^{\,n+1,k} + DD_{wi,j}P_{wi-1,j}^{\,n+1,k} + EE_{wi,j}P_{wi,j}^{\,n+1,k} +$$

$$FF_{wi,j}P_{wi+1,j}^{\,n+1,k} + HH_{wi,j}P_{wi,j+1}^{\,n+1,k} - \left(\frac{\phi}{B_w}\frac{\partial S_w}{\partial P_c}\right)\frac{1}{\Delta t}P_{oi,j}P_{wi,j}^{\,n+1,k} +$$

$$Q_{wi,j}^{\,n+1,k} - \left(\frac{\phi}{B_w}\frac{\partial S_w}{\partial P_c}\right)\frac{1}{\Delta t}P_{wi,j}^{\,n} + \left(\frac{\phi}{B_w}\frac{\partial S_w}{\partial P_c}\right)\frac{1}{\Delta t}P_{oi,j}^{\,n}$$

$$= -R_{wi,j}^{\,n+1,k} \quad \text{.....} \qquad (2f)$$

An equation similar to (2f), can be written for the oil phase. When the equations for two phases are combined, they take the form:

$$B_{i,j}\Delta P_{i,j-1}^{n+1,k+1} + D_{i,j}\Delta P_{i-1,j}^{n+1,k+1} + E_{i,j}\Delta P_{i,j}^{n+1,k+1} + F_{i,j}\Delta P_{i+1,j}^{n+1,k+1} + H_{i,j}\Delta P_{wi,j+1}^{n+1,k+1} = -R_{i,j}^{n+1,k} \quad \text{..... .....} \quad (2\text{ g})$$

Equation (2 g) applied to every grid point in a system with I grids in the x-direction and J grids in the y-direction results in I x J equations, whose coefficients arranged in matrix form, form a penta diagonal matrix as in equation (2 h)..

$$\begin{bmatrix} E_{1,1} & F_{1,1} & H_{1,1} & & & & & & \\ D_{2,1} & E_{2,1} & F_{2,1} & H_{2,1} & & & & & \\ B_{1,2} & D_{1,2} & E_{1,2} & F_{1,2} & H_{1,2} & & & & \\ & B_{i,j} & D_{i,j} & E_{i.j} & F_{i,j} & H_{i,j} & & & \\ & \ddots & \ddots & \ddots & \ddots & & & & \\ & & \ddots & \ddots & \ddots & F_{I,J} & & & \\ & & & \ddots & \ddots & \ddots & & & \\ & & & & B_{I,J} & D_{I,J} & E_{I,J} & & \end{bmatrix} \begin{bmatrix} \Delta P_{1,1} \\ \Delta P_{2,1} \\ \vdots \\ \Delta P_{1,2} \\ \Delta P_{i,j} \\ \vdots \\ \vdots \\ \vdots \\ \Delta P_{I,J} \end{bmatrix} = \begin{bmatrix} -R_{1,1} \\ -R_{2,1} \\ \vdots \\ -R_{1,2} \\ -R_{i,j} \\ \vdots \\ \vdots \\ \vdots \\ -R_{I,J} \end{bmatrix} \quad . (2\text{ i})$$

Where,

$$\Delta P_{i,j} = \begin{bmatrix} \Delta P_{wi,j}^{n+1,k+1} \\ \Delta P_{oi,j}^{n+1,k+1} \end{bmatrix} \quad (2\text{ i. 1})$$

$$-R_{i,j} = \begin{bmatrix} -R_{wi,j}^{n+1,k+1} \\ -R_{oi,j}^{n+1,k+1} \end{bmatrix} \quad (2\text{ i. 2})$$

$$B_{i,j} = \begin{bmatrix} BB_{wi,j} & 0 \\ 0 & BB_{oi,j} \end{bmatrix} \quad (2\text{ i. 3})$$

$$D_{i,j} = \begin{bmatrix} DD_{wi,j} & 0 \\ 0 & DD_{oi,j} \end{bmatrix} \quad (2\text{ i. 4})$$

$$E_{i,j}=\begin{bmatrix} -\left(BB_{wi,j}DD_{wi,j}+FF_{wi,j}+HH_{wi,j}-\left(\frac{\phi}{B_w}\frac{\partial S_w}{\partial P_c}\frac{1}{\Delta t}\right)\right) & -\left(\frac{\phi}{B_w}\frac{\partial S_w}{\partial P_c}\frac{1}{\Delta t}\right) \\ -\left(\frac{\phi}{B_o}\frac{\partial S_w}{\partial P_c}\frac{1}{\Delta t}\right) & -\left(BB_{oi,j}+DD_{oi,j}+FF_{oi,j}-\left(\frac{\phi}{B_o}\frac{\partial S_w}{\partial P_c}\frac{1}{\Delta t}\right)\right) \end{bmatrix} \quad (2\,i.5)$$

$$F_{i,j}=\begin{bmatrix} FF_{w\,i,j} & 0 \\ 0 & FF_{o\,i,j} \end{bmatrix} \quad (2\,i.6)$$

$$H_{i,j}=\begin{bmatrix} HH_{w\,i,j} & 0 \\ 0 & HH_{o\,i,j} \end{bmatrix} \quad (2\,i.7)$$

The absolute permeability $k_{i+1/2,j}$ is expressed as a harmonic mean between the i [th] and (i+1) [th] grid blocks.

$$k_{i+1/2,j}=\frac{2k_{i,j}k_{i+1,j}}{\left(k_{i,j}+k_{i+1,j}\right)} \quad (2\,i.8)$$

The relative permeability $k_{rwi+1/2,j}$ is weighed as:

$$k_{rw\,i+1/2,j}=w\,k_{rw\,i,j}+(1-w)k_{rw\,i+1,j} \quad (2\,i.9)$$

Where, w is some weighing factor. W was arbitrarily taken as 1/2 in the model, so that $k_{rw\,i+1/2\,,\,j}$ can be expressed as:

$$k_{rw\,i+1/2,j}=\frac{k_{rw\,i,j}+k_{rw\,i+1,j}}{2} \quad (2\,i.10)$$

which is the arithmetic average of the two values of the relative permeability in the blocks i and (i+1). A similar treatment is given to the values of the oil relative permeability.

Equation (2 i) is arranged in the form that can be solved by the strongly implicit procedure (SIP) relaxation method of [4]. SIP was used in this study. Details of SIP can be found in the original work.

3.0 DATA USED FOR THE STUDY

3.1 Porous slab

Length : 40cm
Width : 40cm
Thickness: 1.0cm
Porosity 0.375 fraction
Absolute permeability: Varied between 0.5 and 9.28
Relative permeability curves: Figure 1
Capillary pressure curve: Figure 1

3.2 Fluid properties

Water:
B w : 1.0
Viscosity: Varied between 1.5 and 5.0 centipoises
Initial water saturation: 0.125 or 0.25
Initial water pressure: 0.5 and 10 atmosphere
Oil:
B o : 1.0
Viscosity: 1.0 centipoise
Initial oil pressure is computed by the computer program.

3.3 Rate of water injection : 0.0015cc per second per unit volume
Dimensions of grid blocks: 4.0 cm by 4.0 cm

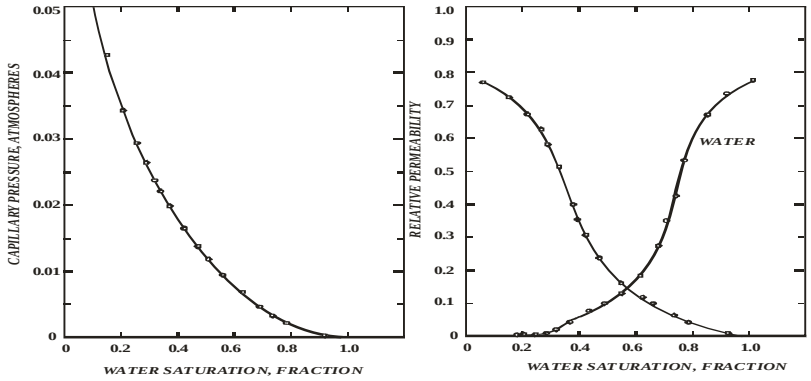

Figure 1: Capillary and Relative Permeability Curves used for the first part of this study

3.4 Selection of the size of time step and grids

In order to save computer time, the time step size (Δt) of 20sec was used together with the injection rate of 0.0015 cc/unit volume the space increment values (Δx and Δy) were set at 4.0cm. The use of this large time step was made possible due to the semi-implicit consideration of the water and oil mobilities. To see if the computation was stable at this value of Δt , a smaller time step (10 seconds) was used to re-run the program while keeping the same values of Δx and Δy. Water saturation profiles from the two runs matched very closely. The compassion is shown in Figure 2. The dimensionless distance in Figure 2 is obtained as follows:

Let I represent the total number of grid y direction; then

Dimensionless distance in x direction = $\frac{x_i}{I\Delta x}$

Where $x_i = 0, \Delta x, 2\Delta x, 3\Delta x, \ldots\ldots\ldots\ldots I\Delta x$

and dimensionless distance in y direction = $\frac{y_i}{J\Delta y}$

where, $y_i = 0, \Delta y, 2\Delta y, 3\Delta y, \ldots\ldots\ldots\ldots J\Delta y$

The small values of Δx and Δy were chosen in order to reduce the numerical dispersion present in numerical computations. The value of 4.0cm was chosen after a run had been made with Δx and Δy taken as 8.0cm. The saturation distribution for the case of grid size of Δx and Δy equal to 8.0cm looked different from the case of Δx and Δy equal to 4.0cm. Numerical dispersion of the case of Δx and Δy equal to 4.0cm was considered acceptable after comparing the results from the program with those obtained by the Buckley-Leverett method in the linear flow case.

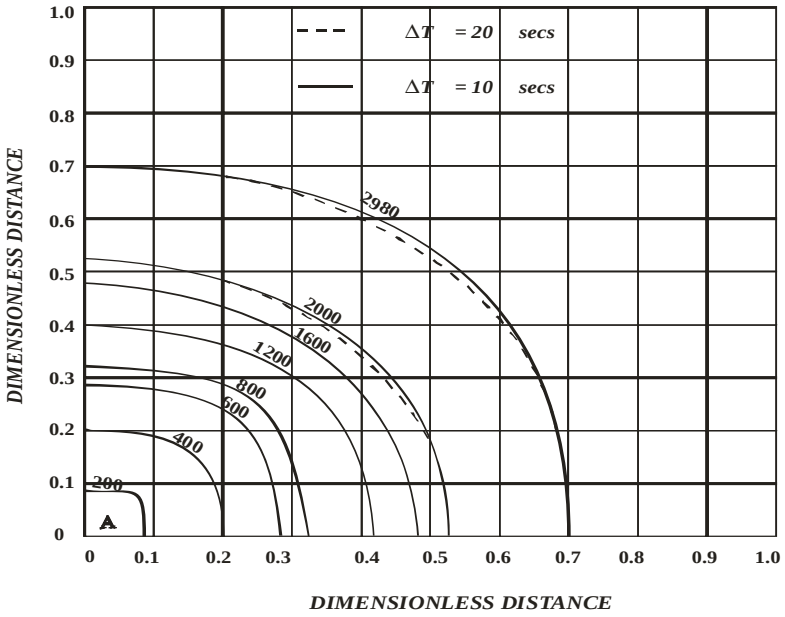

Figure 2: Comparison of saturation contours for two values of time step

4.0 Evaluating The Effects Of A Parameter

In order to evaluate the effects of a chosen parameter on the shape of the water saturation profiles, the time of water breakthrough and the cumulative recovery, a standard run was made with a chosen value of the parameter of interest. By making other runs with an altered value of the parameter and comparing results with that of the standard run, the effect of the required parameter can be visualized. The various comparisons made are described below.

4.1 Studies With The Linear Model.

Although capillary forces are not considered in the Buckley-Leverett method, we can have some idea on the accuracy of the results from the program by comparing them with corresponding values computed by the use of the Buckley-Leverett [2] method.

The integrated form of the Buckley-Leverett equation is:

$$W_i = \frac{L\phi A}{\left.\frac{dF_W}{dS_W}\right|_S} \qquad \ldots\ldots\ldots\ldots\ldots\ldots\ldots\ldots\ldots\ldots \qquad (3.1)$$

where

W_i = total amount of water entering the system

L = total length of the system

S = subscript denoting shock front

Figure 3 shows the graphs of F_w and dF_w/dS_w versus S_w.by use of data shown in Fig. 1

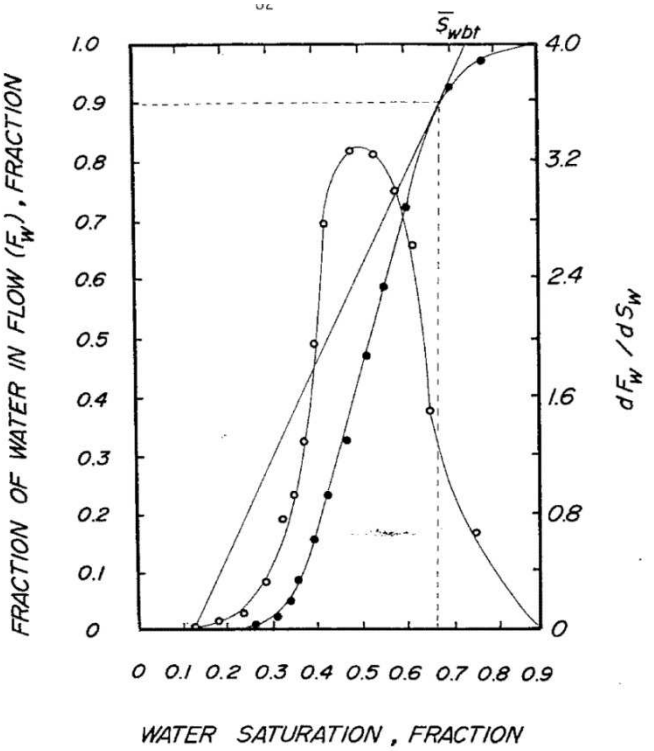

Figure 3: Graphs of F_w and dF_w / dS_w versus Water Saturation (S_w)

W_i was obtained from evaluation by evaluation of equation 3.1 as:

$$W_i = \frac{0.375 \times 4 \times 40}{1.627} = 36.7cc$$

The average water saturation at the time of water breakthrough (S_{wbt}) is read from Fig xxx as 0.73. Results from the program show that breakthrough of water occurs after 36.48cc of water have been injected into the slab. At this stage, the water saturation in the production block was 0.569 (fraction) and the average saturation behind the production block was calculated as 0.639 (fraction). The amount of water injected (W_i) from this study is close to the corresponding value obtained by the Buckley-Leveret method but there is disparity between the corresponding values of S_{wbt}.

Equation (3.1) can be rearranged to solve for the distance a plane of fixed saturation moves (X_{Sw}) after some known of water has been injected into the system:

$$X_{SW} = \frac{W_i}{\phi A}\left(\frac{dF_W}{dS_W}\right)S_W \qquad \ldots\ldots\ldots\ldots\ldots\ldots\ldots\ldots \qquad (3.2)$$

The various values of X_{SW} are plotted against S_W together with saturation profile from the program in Fig 4 where the disparity between the shock front saturation and the average water saturation behind the front obtained Leverett method and those from the study is clearly shown.

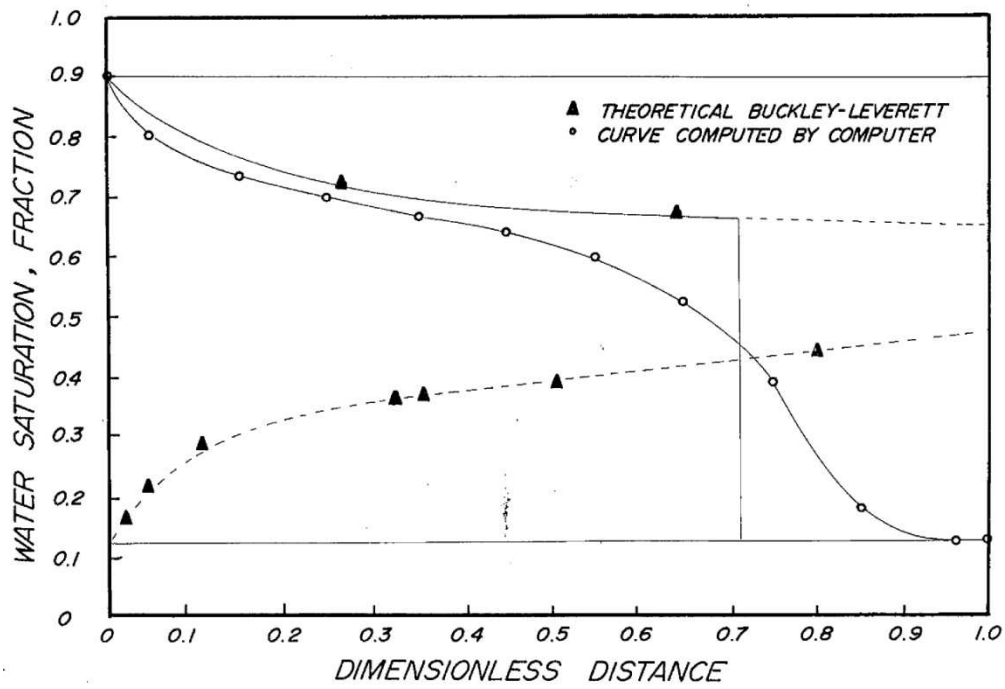

Figure 4: Disparity between shock front profile of Buckley-Leveret and that of this study.

Effect of water to oil viscosity ratio

The linear model was used to study the effect of water to oil viscosity ratio. The ratio was set at 1 for the standard run. Another run with the ratio set at 1.5 was made. Figure 5 shows corresponding profiles for the second case. Figure 6 shows cumulative oil production from the two cases plotted together.

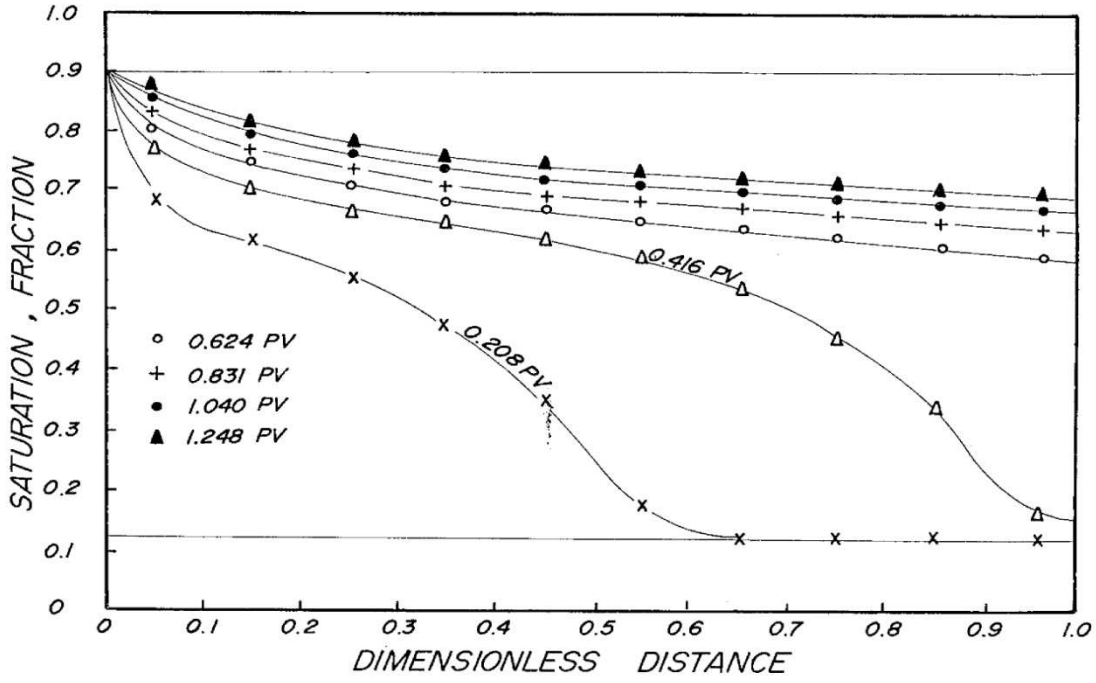

Figure 5: Saturation Distribution (Water / Oil viscosity ratio=1.0) at various values of cumulative Water injection

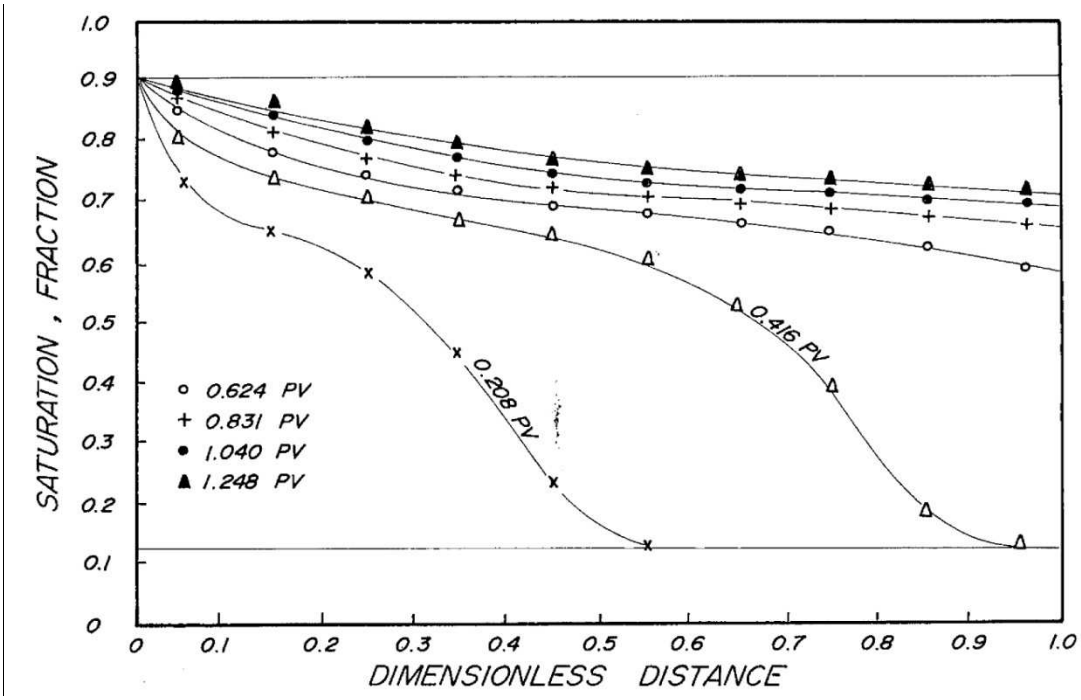

Figure 6: Saturation Distribution (Water / Oil viscosity ratio=1.5) at various values of cumulative Water injection

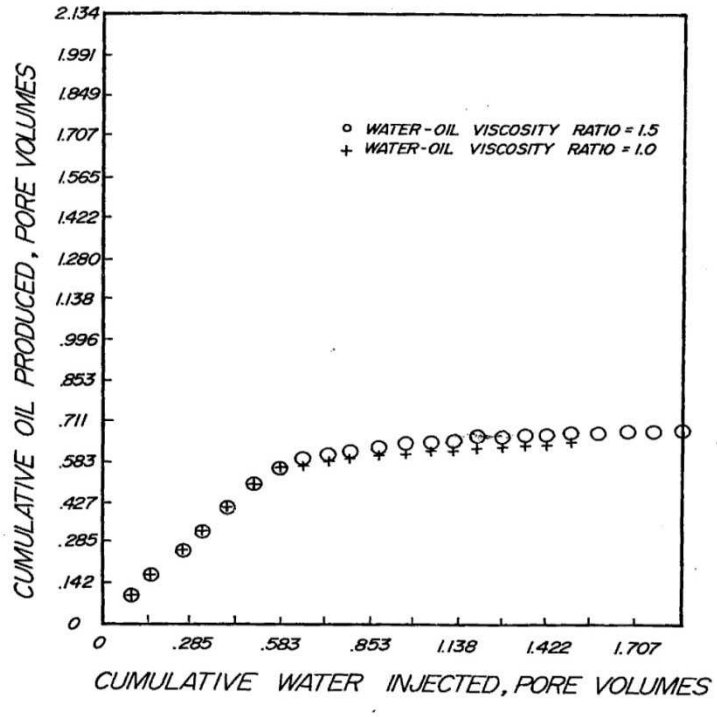

Figure 7: Effect of changing Water / Oil viscosity on cumulative Oil Recovery (results from linear model)

4.2 Studies With The Five Spot Model

Studies with the five spot water flood pattern were conducted with two sets of capillary and relative permeability curves. The first set of curves is that shown in Figure 1. This set of curves was also used for the linear study. The second set of curves is shown in Figure 14. Studies with this set of curves are discussed where the Figure is presented. The curves in Figure 1 were used for the standard run. Other data used for the standard run are:

The data for the standard run for studies with the five spot models are:

Absolute permeability:	9.28 darcys
Connate water saturation:	12.5 percent
Water-to-oil viscosity ratio:	1.5

It took 13120 seconds to water out the slab in the standard run and material balance figures were in the range 0.992917 – 1.00623.

Table 1 shows the effect of various properties of a five spot water flood on the cumulative oil production by the use of the first set of capillary and relative permeability curves. The properties considered are

1. Connate water saturation
2. Water to oil viscosity ratio
3. Anisotropy
4. Equal water injection at four connects of the five spot
5. Unequal water injection at four connects of the five spot
6. Shape of Capillary and relative permeability curves

The stared (***) values in Table 1 are runs in which the porous slab was completely watered out. That is; maximum water saturation was attained in all grid blocks.

4.2.1 Effect of connate water saturation

A run with connate water saturation of 25 percent was made. Fig 8 shows the saturation contours from this run with compared with those from the standard run. Table 1 shows cumulative oil recovery data for various runs including this case. The Table shows that breakthrough will occur earlier in this case and that more oil will be recovered from the standard run. For the Run shown in Figure 8, material balance ranged from 0.9920990 to 1.000623, over the duration of 10560 seconds it took to water out the slab.

Table 1: Cumulative Water injected versus cumulative Oil produced for various Five Spot Runs by use of the first capillary and relative permeability curves

CUMULATIVE WATER INJECTED, PORE VOLUMES	**CUMULATIVE OIL PRODUCED, PORE VOLUMES**								
	k: 9.28 $\frac{\mu_W}{\mu_o}$:1.5 S_{wc}: 0.125	k: 9.28 $\frac{\mu_W}{\mu_o}$:1.5 S_{wc} : 0.25	k: 9.28 $\frac{\mu_W}{\mu_o}$: 5.0 S_{wc} 0.125	k: 1.0 $\frac{\mu_W}{\mu_o}$:1.5 S_{wc}: 0.125	k: 0.5 $\frac{\mu_W}{\mu_o}$:1.5 S_{wo}:0.125	$\frac{\mu_W}{\mu_o}$:1.5 S_{wo}:0.125 Alternating sequence of k: 1.0 & k: 0.5	$\frac{\mu_W}{\mu_o}$: 1.5 S_{wo}:0.25 Anisotropy kx: 9.28 ky: 0.928	Five spot with equal water injection at four corners k:9.28 $\frac{\mu_W}{\mu_o}$: 1.5 S_{wo}:0.25	Five spot with un-equal injection at four corners k:9.28 $\frac{\mu_W}{\mu_o}$: 1.5 S_{wo}:0.125
(I)	(II)	(III)	(IV)	(V)	(VI)	(VII)	(VIII)	(IX)	(X)
0.0400	0.0400	0.0397	0.0400	0.0400	0.0400	0.0400	0.0397	0.0397	0.0397
0.0800	0.0799	0.0793	0.0800	0.0799	0.0799	0.0799	0.0793	0.0793	0.0793
0.1600	0.1599	0.1599	0.1600	0.1599	0.1599	0.1599	0.1599	0.1599	0.1642
0.2002	0.2000	0.1956	0.2002	0.2001	0.1999	0.1977	0.1956	0.1956	0.1979
0.2400	0.2399	0.2353	0.2400	0.2399	0.2399	0.2399	0.2379	0.2337	0.2336
0.2800	0.2799	0.2667	0.2800	0.2800	0. 2798	0.2798	0.2752	0.2638	0.2652
0.3200	0.3198	0.2938	0.3200	0.3198		0.3198	0.3172	0.2915	0.2938
0.3600	0.3520	0.3176	0.3600	0.3598		0.3577	0.3492	0.3108	0.3143
0.4000	0.3927	0.3378	0.4000	0.3997		0.3997	0.3898	0.3371	0.3374
0.4224	0.4082	0.3481***	0.4224	0.4220		0.4225	0.4051	0.3449	0.3484
0.4240	0.4089		0.4240	0.4240		0.4237	0.4057	0.3463	0.3499

0.4400	0.4207		0.4399	0.4397				0.3477	0.3513
0.4800	0.4446		0.4799	0.4797				0.3663	0.3698
0.5040	0.4570		0.4978	0.4978				0.3733	0.3762
0.5200	0.4644		0.5199	0.5197				0.3804	0.3819
0.5248	0.4669***		0. .5191	0.5148				0.3826	0.3840
0.5520			0.5376	0.5486				0.3890	0.3918
0.5600			0.5571					0.3911	0.3947
0.5648			0.5611					0.3925	0.3961
0.6000								0.4004	0.4018
0.8000								0.4347	0.4378
0.9600								0.4557	0.4594
1.0000								0.4608	0.4629
1.0680								0.4686	0.4698 ***
1.1200								0.4742	
1.2800								0.4918	
1.5840								0.5254***	

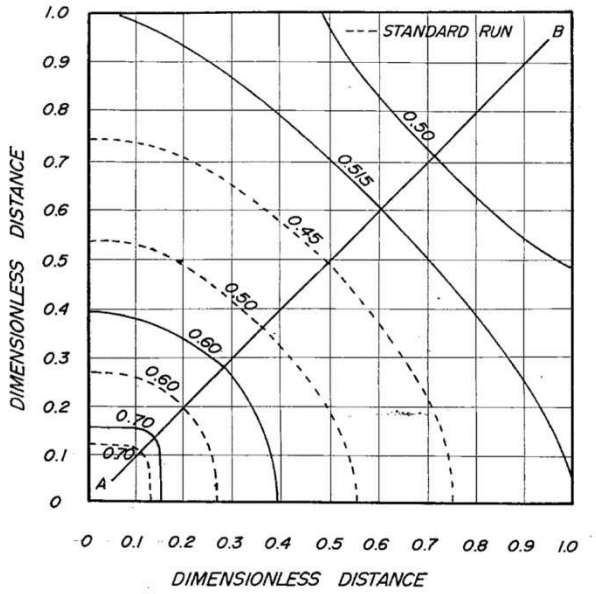

Figure 8: Comparison of saturation contours after cumulative water injection of 0.320 pore volumes with corresponding contours of the standard run. Solid lines are for the case of 25 % connate water saturation

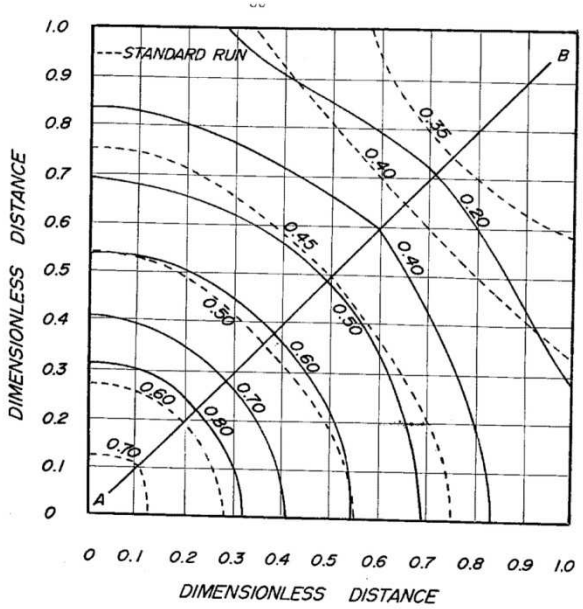

Figure 9: Comparison of saturation contours after cumulative water injection of injection of 0.320 pore volumes with corresponding contours of the standard run. Solid lines are for the case of 5.0

4.2.2 Effects of water-to-oil viscosity ratio

Fig 9 shows that comparison of saturation contours from a run with water-to-oil viscosity ratio equal to 5.0 with those of the standard run. From this figure and Table 1, we observe that more oil would be recovered (for any given pore volume of water injected) from the present case than from the standard run. Also, more time is required to water-out the slab in this case of favorable mobility ratio. Material balance was in the range 0.944608 – 1.000443 and slab was not completely watered out.

4.2.3 Effects of Anisotropy

In this run, the value of absolute permeability in the x direction (kx) was set at 9.28 darcys and that in the y direction (ky) at 0.928 darcys. The saturation profiles after 0.32 pore volumes of water have been injected into the system are shown in Figure 10. The diagram shows direction of flow favoring the x direction as streamlines search for the path of least resistance. Figure 11 reveals the contrast between the diagonal cross- sections of the anisotropic case and the corresponding cross-sections from the standard run. Cumulative oil recovery from the anisotropic case is also shown in Table 1. From the Table, it is seen that the cumulative oil recovery from the anisotropic case is less than corresponding recoveries from the standard run (at a given value of cumulative water injection).

Range of material balance was 0.991456 to 1.000380 over 10600 the program was executed.

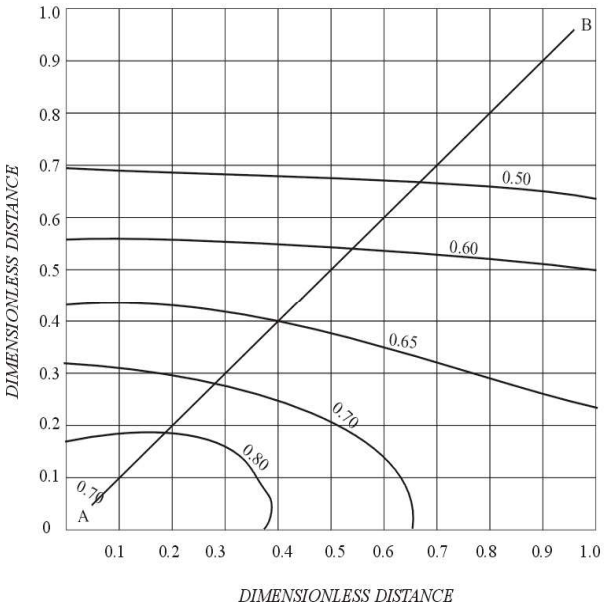

Figure 10: Saturation contours at cumulative water injection of 0.320 pore volumes for the anisotropic case.

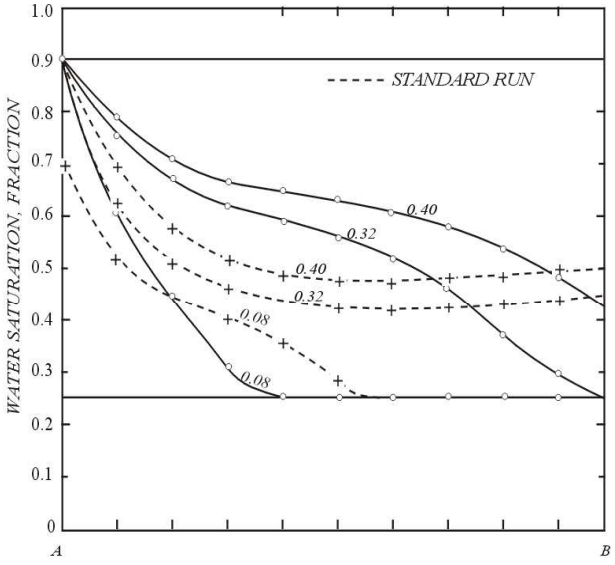

Figure 11: Cross-section a – b for three values of cumulative water injection (pore volumes) compared with corresponding cross-sections of standard run. Solid lines are for anisotropic case.

4.2.4 Effects of taking a five-spot with equal injection at four corners

In this run, the rates of water injection at the four corners of the pattern were considered equal and were set at 0.0015 cc / sec per unit volume of the injection block at each corner. Production rate from the centre of the slab was set equal to the sum (that is, 0.0060 cc / sec per unit volume of the cell block) of the amount injected at each of the four corners. Figure 12 shows the water saturation profiles after injecting 0.32 pore volumes of water into the system. The figure shows a four-fold symmetry that is expected of it. The connate water saturation from this case was 25% so that the standard run for comparison is the quadrant injection with 25% connate water saturation.

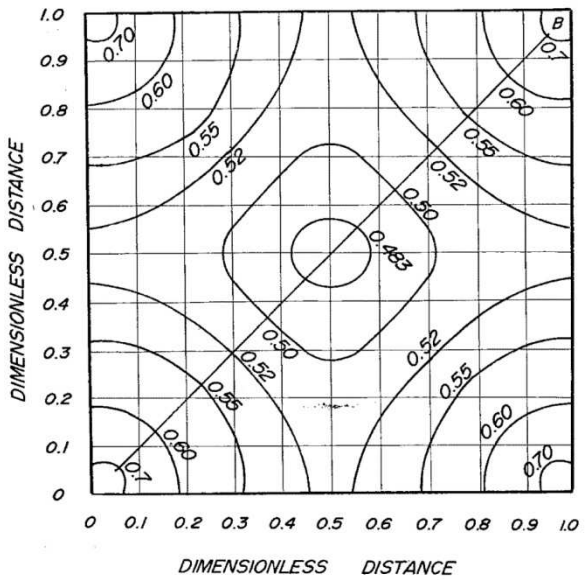

Figure 12: Saturation contours at cumulative water injection of 0.320 pore volumes. Case of Five –Spot with equal rate of injection (0.0015 cc / sec) at the four corners.

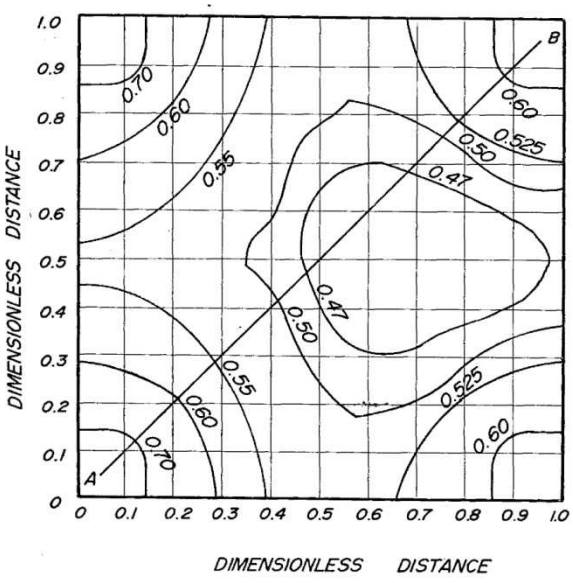

Figure 13: Saturation contours at cumulative water injection of 0.320 pore volumes. Case of Five –Spot with unequal rate of injection at the four corners.

Table 1 shows that breakthrough occurs earlier in this case than for the standard run. It also shows that more oil will be recovered in this case. Both effects could be due to closer well spacing resulting in higher flushing rate. Another deduction from Table 1 is that more oil is produced beyond breakthrough in this case than for the standard run. 1.584 pore volumes are required to water out this system as against the 0.422 pore volumes required by the standard run. Maximum water saturation in the production block was 67.46% for this case while it was 54.7% for the standard run. The average water saturation at the time of complete flushing was 68.4%. This value of water saturation is closer to the expected field residual oil saturations (from water flooding) which usually range between 25 and 40 percent. Material balance was in the range 0.960258 – 1.000000 over 9900 seconds it took to water out the slab. This shows a fair accuracy. Another advantage of the present configuration is that it can be used to study the field case where water is injected at unequal rates into the various wells.
This case of unequal injection is considered next.

4.2.5 Effects of taking a five-spot with unequal injection at four corners

In this run, the injection rates at each of the left hand corners was 0.0030 cc / sec per unit volume of the injection block while that at each of the right hand corners, 0.0015 cc / sec per unit volume of the injection block.

Saturation contours after 0.32 pore volumes of water have been injected into the slab are shown in Figure 13. There is no longer symmetry of saturation contours.

Cumulative oil recovery data for this case are also shown in Table 1. Cumulative oil recovery at any stage of water injection (before the slab is watered out in the present run) is higher in this case as compared with the case of equal injections at the four corners. However, in the present case, the slab is watered out much sooner. It took 5340 seconds to water out the slab and material balance figures were in the range 0.998650 – 1.003800. This results in less overall recovery in the present case compared to the case of equal injection rates.

4.2.6 Effects of the shape of relative permeability and capillary pressure curves

The relative permeability and capillary pressure curves shown in Figure 14 (also called the second set of Capillary and Relative Permeability curves at the beginning of this section), were used for this run, and the slab was considered as a quadrant of a five-spot with one injection well and one production well.

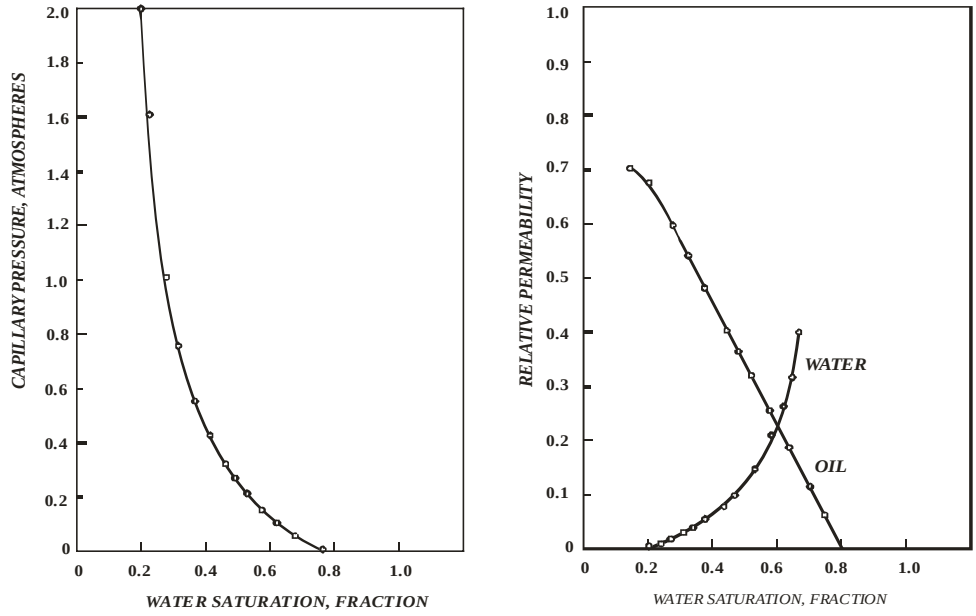

Figure 14: Effect of shape of Capillary and Relative Permeability Curves.

Because of the fairly high capillary pressure, the initial water pressure was set at 10 atmospheres and the initial water saturation at 25%. Other data were as for the five-spot with 25% connate water saturation and that run was used as the standard for comparison. A comparison of saturation contours from this case with those from the standard run is shown in Figure 15.

The Figure shows that water travelled faster in this case than for the standard run. A comparison of diagonal profiles is shown in Figure 16. The profiles from the present case are almost flat, indicating the absence of a 'shock-front'. The absence of the front was confirmed by the shape of the fractional flow curve of the Buckley-Leverett analysis not shown in this paper.

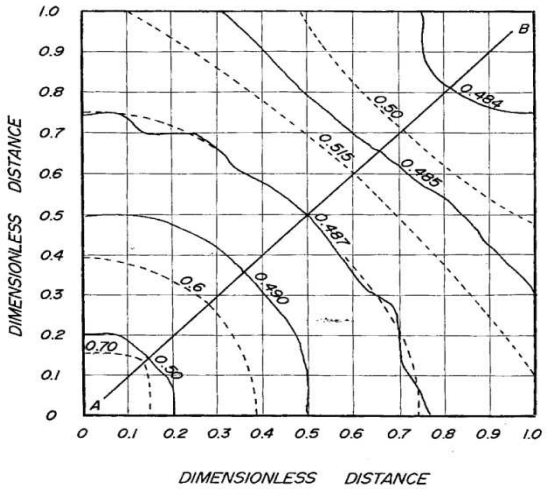

Figure 15: Comparison of saturation contours at cumulative water injection of 0.320 pore volumes with corresponding contours of the standard run. Solid lines are for case with different set of capillary and relative permeability curves

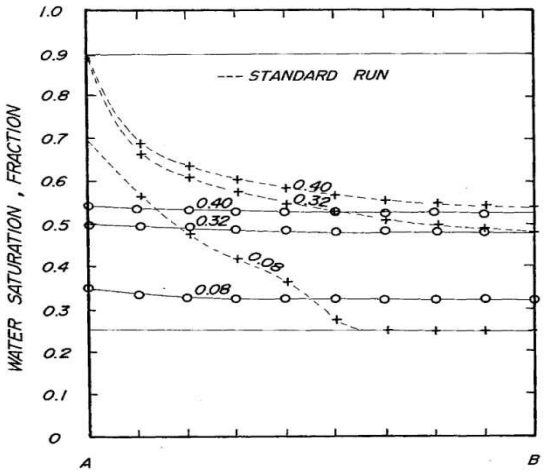

Figure 16: Cross-section a – b for three values of cumulative water injection (pore volumes) compared with corresponding cross-sections of the standard run. Solid lines are for case with different set of capillary and relative permeability curves

Cumulative oil recovery from this case is shown in Table 2 together with the corresponding value from the standard run. The table shows that there is more oil recovered from this case than from the standard run after a cumulative water injection of 0.40 pore volumes into both slabs.

Table 2: Effect of shape of relative permeability and capillary pressure curves on certain properties of a five-spot water flood

PROPERTIES COMPARED	**FIRST SET OF DATA** **k: 9.28 DARCYS** $\frac{\mu_W}{\mu_o}$: 1.5 **INITIAL S_W: 0.250 FRACTION**	**SECOND SET OF DATA** **k: 9.28 DARCYS** $\frac{\mu_W}{\mu_o}$:1.5 **INITIAL S_W: 0.250 FRACTION**
Cumulative water injected, pore volume	0.400	0.400
Cumulative oil produced, pore volume	0.338	0.361
Water saturation at production block at total time considered	0.539589	0.527060
Total time considered	10,000 seconds	10,000 seconds
Range of material balance	0.991090-1.000623 over 0.4224 pore volumes	0.785118-1.003592 over 0.4720 pore volumes

It also shows that water saturation in the production block at 0.4 pore volumes of water injection is 52.71 percent in the present case while it is 53.96 percent in the standard run. The value of the water saturation for the present case should be higher (since more oil has been recovered from it than in the standard run). A further evidence of the poor accuracy of the results from this case is seen in the poor range of material balance exhibited by this run. The material balance range is 0.785118-1.003592. The poor accuracy is be due to the unusual shape of the oil relative permeability data – it is almost a straight line throughout its entire length.

Conlusions

The conclusions made from the entire study are as follows:

1. The mathematical model used in this report is able to predict oil recovery form a water flood project with reasonable accuracy. This accuracy was ascertained by comparing the results of the linear model form this study with analytical results obtained by the method of Buckley and Leverett. Also the water saturations obtained at the time the slab is watered- out conform to the general trend observed in the field for the five-spot pattern of water flooding.
2. The model used in this report is well applicable to anisotropic reservoirs.
3. Oil recovery form water flooding with high ratio of water-to-oil viscosity is higher for the same pore volumes of water injected than in the case of the less favorable ratio.Even though, the ultimate volume oil that can be recovered from the system will have to be the same in both cases.
4. A high value of initial water saturation will result in less cumulative oil recovery (at any given pore volumes of water injected) into the system. However, less pore volumes of water (hence time) are required to flood-out the reservoir.
5. In stimulating a five spot pattern water flood, it might be better to consider the five-spot with injection at four corners and taking production from the central well than to consider a quadrant of the five-spot with one injection well and one production well. Also, the five-spot with four injection wells can be used to simulate flooding with unequal injection rates whereas; the quadrant representation cannot be used.

REFERENCES

1. Craig, F. F. Jr., Caudle, B.H. Mungan, N., Johansen, R. T., Poetmann, F.H. , Crawford, P.B., and Farouq Ali, A.M. (1974): “Secondary and tertiary Oil Recovery Processes”, Interstate Oil Compact Commission.
2. Pirson, S. J.(1977) Oil Reservoir Engineering, Robert E. Krieger Publishing company, New York.
3. Spiegel, M. E. (1971): “Calculus of Finite Differences and Difference Equations, Shaum’s Outline Series, McGraw-Hill Book Company, New York.
4. Stone, H. L. (1968): “Iterative Solutions of Implicit Approximations of Multidimensional Partial Differential Equations”, SIAM J. on Numerical Analysis Vol. 5, 530.
5. Weinstein, H. G., Stone, H.L. Kwan, T. V.: “Simultaneous Solution of Multiphase Reservoir Flow Equations”, Soc. Pet. J. (June, 1970) 99-110.